ELSEVIER

International Journal of Mass Spectrometry 217 (2002) 45–54

International Journal of Mass Spectrometry

www.elsevier.com/locate/ijms

Ionized aniline and its distonic radical cation isomers

Hung Thanh Le [a,c], Robert Flammang [b,1], Monique Barbieux-Flammang [b], Pascal Gerbaux [b], Minh Tho Nguyen [a,*]

[a] *Department of Chemistry, University of Leuven, Celestijnenlaan 200F, B-3001 Leuven, Belgium*
[b] *Organic Chemistry Laboratory, University of Mons-Hainaut, Avenue Maistriau 19, B-7000 Mons, Belgium*
[c] *Group of Computational Chemistry, Faculty of Chemical Engineering, Ho Chi Minh City University of Technology, Ho Chi Minh City, Viet Nam*

Received 4 July 2001; accepted 12 October 2001

Dedicated to the memory of our friend and colleague Pierre Longevialle

Abstract

A multi-sector tandem mass spectrometer fitted with a radiofrequency (rf)-only quadrupole collision cell (Qcell) has allowed fast and unambiguous identification of dehydroanilinium ions, the distonic isomers of ionized aniline. These ions were prepared by collisional deiodonation of protonated iodoanilines previously generated by chemical ionization (CI) or even better by liquid secondary ion mass spectrometry (LSIMS) conditions. Ab initio quantum chemical calculations were also used to probe the protonation of aniline and halogeno-anilines, **X**–C_6H_4–NH_2 (**X** = F, Cl, Br and I) and the relative stabilities of ionized aniline and its distonic radical cation isomers. Proton affinities (PAs) of anilines at nitrogen and carbon sites were found rather dependent on the nature and the position of the substituents. (Int J Mass Spectrom 217 (2002) 45–54)

Keywords: Tandem mass spectrometer; Quantum chemical calculations; Aniline; Distonic radical cations; Proton affinities

1. Introduction

Using Fourier transform ion cyclotron resonance (FT-ICR) experiments, Chyall and Kenttämaa [1,2] convincingly demonstrated the formation of dehydroanilinium ion **b**, a distonic isomer of conventional aniline radical cation **a**.

Structure identification was based on ion–molecule reactions with dimethyl disulfide: the attachment of a methylthio radical, which usually characterized distonic ions [3], was detected for ion **b**, not for ion **a**.

In the present work, we have attempted to obtain further support for these conclusions by using a large scale tandem mass spectrometrer [4] modified by the insertion of a quadrupolar collision cell [5]. One of the unique features of such an instrument is the possibility of studying collisional activation in the *high kinetic energy* (8 keV) *regime* of ions generated during the flight in the mass spectrometer (metastably or collision induced) and the usefulness of such experiments which avoids the drawbacks of the MS/MS/MS methodology, that is low mass resolution and sensitivity, has been proved in several recent works [6]. The experimental findings were consolidated by ab initio quantum chemical calculations. In addition, the protonation process in a series of halogeno-anilines was also considered.

* Corresponding author. E-mail: minh.nguyen@chem.kuleuven.be
[1] Co-corresponding author. E-mail: robert.flammang@umh.ac.be

1387-3806/02/$ – see front matter
PII S1387-3806(02)00530-4

2. Experimental

The spectra were recorded on a large scale tandem mass spectrometer (Micromass AutoSpec 6F, Manchester) combining six sectors of $E_1B_1cE_2qcE_3B_2cE_4$ geometry (E stands for electric sector, B for magnetic sector, c for the collision cells used in the present work and q for a radiofrequency (rf)-only quadrupole collision cell(Qcell)) [4]. General conditions were 8 keV accelerating voltage, 200 μA trap current (in the electron ionization (EI) mode), 1 mA (in the chemical ionization (CI) mode,), 70 eV ionizing electron energy and 200 °C ion source temperature. The solid samples were introduced with a direct insertion probe, while the liquid samples were injected in the ion source via a heated (180 °C) septum inlet. The liquid secondary ion mass spectrometry (LSIMS) experiments were performed with a cesium ion gun (10–15 keV); the samples were dissolved in glycerol acidified with trifluoroacetic acid (1%).

The installation of an rf-only Qcell inside the instrument between E_2 and E_3 has also been reported elsewhere [5]. This modification allows the study of associative ion–molecule reactions and the study of collisional activation of decelerated ions. The experiments utilizing the Qcell consist of the selection of a beam of fast ions (8 keV) with $E_1B_1E_2$ and the deceleration of these ions to approximately 20–30 eV. The interaction between the ions and the reagent gas (the pressure of the gas is estimated to be about 10^{-3} Torr) is thereafter realized in the Qcell and, after re-acceleration at 8 keV, all the ions generated in the quadrupole are separated and mass measured by scanning the field of the second magnet.

The *high energy* CA spectra of mass selected ions generated in the Qcell have been recorded by scanning the field of E_4 after collisional activation (nitrogen) in the last collision cell.

Aniline (**1**), 4-iodoaniline (**2**), 3-iodoaniline (**3**) and 2-iodoaniline (**4**) were commercially available (Aldrich) and used without further purification.

3. Results and discussion

3.1. Collisional activation (MS/MS/MS) experiments

Protonated 4-iodoaniline (*m/z* 220) was readily generated upon CI using methane as the reagent gas. Although, earlier theoretical studies [7,8] disagreed with each other on the regioselectivity of the protonation of unsubstituted aniline, collisional activation in the low or high kinetic energy regimes lends support for the formation of (at least partly) ammonium ions $\mathbf{2H}^+$ (nitrogen protonation), in agreement with earlier experimental MS studies [9,10]. For instance, the collisional activation spectrum of $\mathbf{2H}^+$ recorded with argon in the quadrupole collision cell (Fig. 1a)

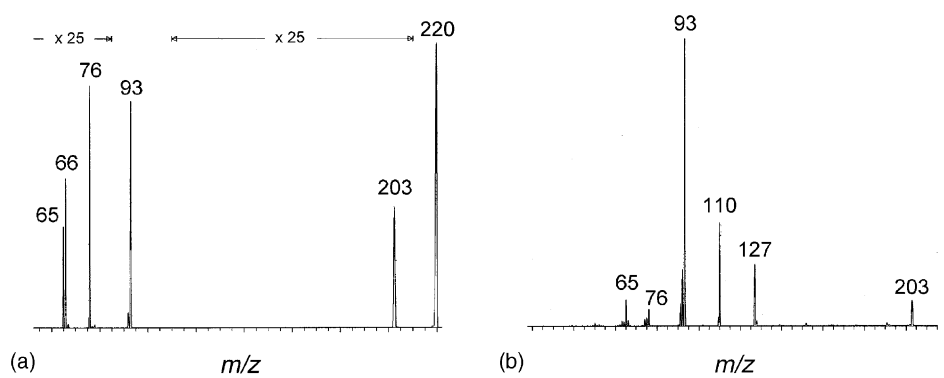

Fig. 1. Collisional activation spectra of protonated 4-iodoaniline $\mathbf{2H}^+$ in the low kinetic energy regime (argon, ca. 20–30 eV) (a) and in the high kinetic energy regime (oxygen, 8 keV) (b).

features, beside the major loss of a iodine atom (*m*/*z* 93), structure-significant peaks at *m*/*z* 203 for the loss of ammonia and *m*/*z* 76 for a consecutive eliminations of NH_3 and $I^{\bullet}$. It is worthy of note that the extremely efficient iodine loss is also a prominent reaction in the high energy CA spectrum of the $\mathbf{2H}^+$ ions (Fig. 1b).

Following isolation of the *m*/*z* 220 ions by using the first three sectors and deceleration from 8 keV to some 20–30 eV, collisional deiodination was performed in the Qcell and the product ions reaccelerated up to 8 keV. Mass selected *m*/*z* 93 products were thereafter collisionally activated with nitrogen collision gas and the resulting CA spectrum is compared in Fig. 2 to the spectrum of "conventional" aniline molecular ions $\mathbf{1}^{\bullet+}$ (ions **a**).

Although, both spectra were found to be quite similar, some structurally significant differences can readily be noticed: (a) a different distribution of the peak intensities in the *m*/*z* 73–78 region, *m*/*z* 76 (loss of NH_3) being favoured for ions **b** and *m*/*z* 77 (loss of NH_2) for ions **a** and an intensification of the peak at *m*/*z* 50 (consecutive loss of ethyne from *m*/*z* 76 ions) for ions **b**. These differences are interpreted as resulting from the production, at least partly, of a non classical dehydroanilinium structure **b** in the dehalogenation process of protonated 4-iodoaniline $\mathbf{2H}^+$ (cf. Scheme 1).

Similar results were obtained with protonated 3-iodoaniline $\mathbf{3H}^+$ and 2-iodoaniline $\mathbf{4H}^+$. Deiodination is again the most intense process upon collisional activation with argon in the Qcell. The CA spectra of

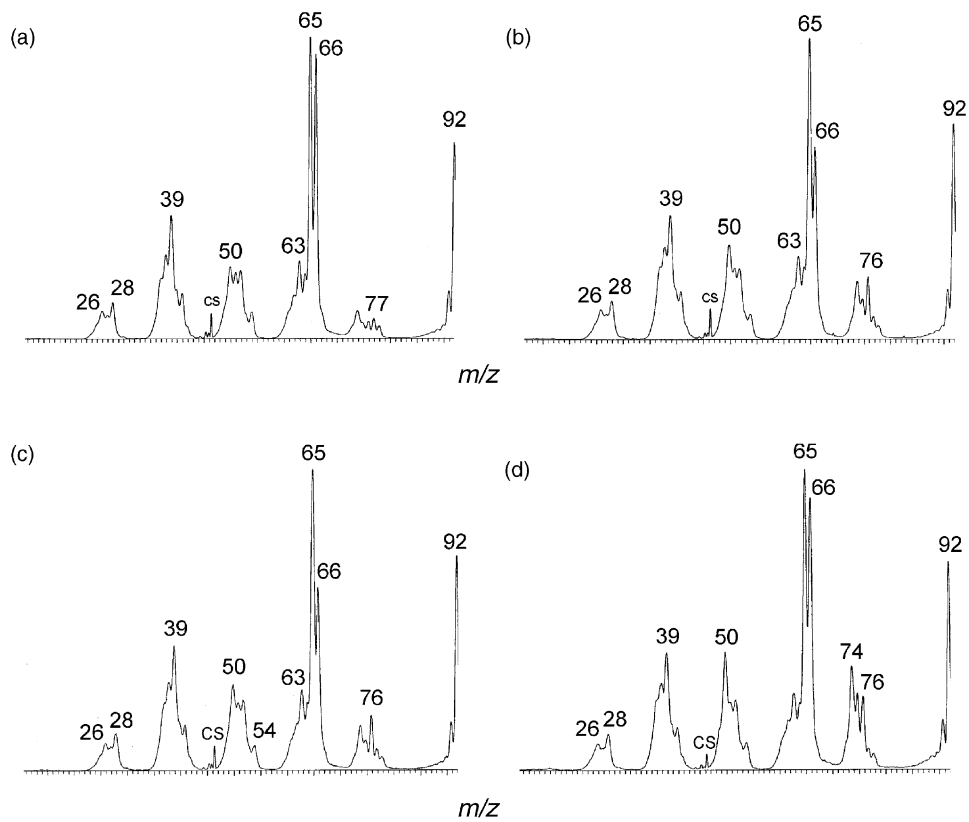

Fig. 2. Collisional activation spectra (nitrogen collision gas) of the *m*/*z* 93 ions produced by EI of aniline (a) and collisional deiodination of $\mathbf{2}$–$\mathbf{4H}^+$ ions within the quadrupole collision cell (argon collision gas) (b–d). CS refers to charge stripping.

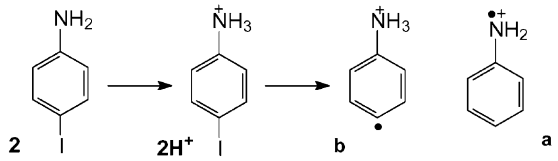

Scheme 1.

the so-produced ions (*m*/*z* 93) (see Fig. 2c and d) are similar but not superimposable to the spectrum of the distonic ions **b** suggesting that isomeric species such as **c** and **d** are formed in the protonation–deiodination reaction sequence (Scheme 2). The most striking features of the CA spectra are again the increased intensity of the peaks at *m*/*z* 76 and 50 and, albeit of very low intensity, a peak at *m*/*z* 17, not detected for aniline molecular ions **a**. The higher intensity of the peak at *m*/*z* 74 is also worthy of note.

Neutralization–reionization (NRMS) experiments have demonstrated that the nitrogen protonation of aniline is dominant under fast atom bombardment (FAB) conditions. That was indicated by the presence of a very weak recovery signal at *m*/*z* 94 in the NR spectrum together with a significant peak at *m*/*z* 17 for reionized ammonia [11]. More recently, *N*-alkylanilines were also shown to be protonated at nitrogen under FAB conditions [12,13]. This chemical behavior can be explained by the fact that ion formation in FAB or LSIMS involves the "vaporization" of ions *preformed* in matrix solution [14] and it is well known that the anilinium ions, stabilized by solvation, are the dominant species in solution [15].

We have therefore, applied the protonation–deiodination sequence to the iodoanilines **2** and **3** using the LSIMS ion source. The high energy CA spectra (Fig. 3) of the $\mathbf{2H}^+$ and $\mathbf{3H}^+$ ions obtained in these conditions are indeed completely different from the spectra shown in Fig. 2 and feature very intense peaks at *m*/*z* 76, 74 and 50. These peaks, that have been associated with the dehydroanilinium structure **b**–**d** in the CI experiments, are those expected for such a distonic ion structure.

In summary, collisional deiodination of protonated iodoaniline is proven to be a very efficient reaction which produces hydrogen shift (distonic) isomers of aniline molecular ions, especially when the ions are produced under LSIMS conditions. This is evidenced by the study of the high energy CA spectra of these ions. It is worthy of note that these spectra were obtained for 8 keV *ions* although the distonic ions were collisionally prepared by loss of iodine. This constitutes one of the unique features of our hybrid tandem mass spectrometer.

3.2. Quantum chemical calculations

Having confirmed the existence of the distonic radical cation isomers of ionized aniline, we have set out to determine some useful quantitative parameters regarding the protonation and ionization of anilines making use of ab initio quantum chemical computations. Calculations were performed on various ionized forms of aniline and protonated halogeno-anilines by means of the Gaussian 98 suite of programs [16]. Geometries were optimized using density functional theory (DFT) at the B3LYP/6-31G(d,p) level, electronic energies were subsequently obtained by single point B3LYP calculations with a larger 6-311++G(d,p) basis set and corrected for harmonic vibrational zero-point energies at the B3LYP/6-31G(d,p) level. Basis set having similar quality but including effective core potential [17] were applied to iodine atom in all calculations of

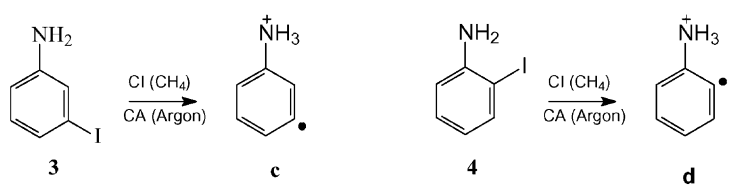

Scheme 2.

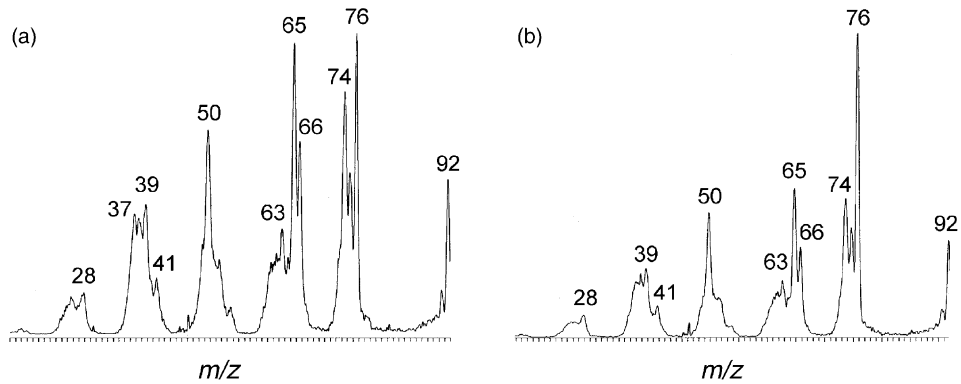

Fig. 3. Collisional activation spectrum (nitrogen collision gas) of the *m/z* 93 ions produced by collisional deiodination of $\mathbf{2H}^+$ (a) and $\mathbf{3H}^+$ (b) ions produced in LSIMS conditions.

iodoanilines. In order to probe further the protonation sites, ab initio molecular orbital calculations using the MP2 and CCSD(T) methods with the 6-311++G(d,p) and 6-311++G(3df,2p) basis sets have also been employed for the parent aniline, whereas the MP2 computations based on HF optimized geometries were applied for substituted anilines.

3.2.1. Protonation of aniline and halogeno-anilines

3.2.1.1. Aniline. Calculated proton affinities (PAs) of aniline in the gas phase are collected in Table 1. Due to the fact that the *meta*- and *ortho*-carbons of the phenyl ring is proven to be the least favoured sites in the electrophilic reaction, we have considered only the nitrogen and *para*-C_4 carbon sites. The results are in agreement with recent theoretical studies [7,8]. While the MP2 and CCSD(T) methods indicate that nitrogen is the most susceptible site to a proton attack, the DFT B3LYP method indicates a protonation at the carbon-C_4 (see Scheme 3 for atom numbering). In comparison with the available experimental values of 877 kJ/mol [18] and 874 kJ/mol [19], both B3LYP and CCSD(T) methods with the 6-311++G(3df,2p) basis set give good results for the PA(N) namely 874 and 877 kJ/mol, respectively. The MP2 and B3LYP models in conjunction with the smaller 6-311++G(d,p) basis set also provide comparable results, being 878 and 874 kJ/mol, respectively.

A discrepancy between results obtained using DFT and standard molecular orbital theory appears in the case of carbon-C_4 protonation in which the corresponding proton affinity (PA)(C_4) estimated by B3LYP/6-311++G(3df,2p) is higher by 8 kJ/mol than the PA(N), whereas the PA(C_4) value calculated using CCSD(T) method with the same basis set turns out to be 7 kJ/mol lower with respect to the PA(N). In this case, it is clearly difficult to say which method should

Table 1
Calculated PA (kJ/mol) at 0 K of aniline from different methods

Method[a]	PA(N)	PA(C_4)
B3LYP/6-311++G(d,p)	874	882
B3LYP/6-311++G(3df,2p)	874	882
MP2/6-311++G(d,p)	878	851
MP2/6-311++G(3df,2p)	868	843
CCSD(T)/6-311++G(d,p)	886	879
CCSD(T)/6-311++G(3df,2p)	877	870

[a] Based on B3LYP/6-311++G(d,p) optimized geometries. Zero-point energies from B3LYP/6-31G(d,p). Experimental values: 877 kJ/mol [18] and 874 kJ/mol [19].

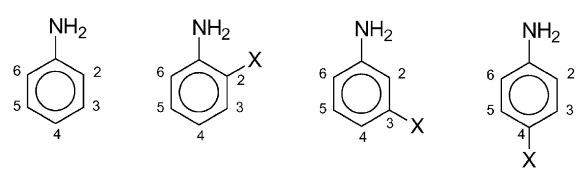

Scheme 3.

be the more reliable one. Moreover, experimental results on the site of protonation of aniline have still been not clear-cut. While some authors suggested a protonation on the ring carbons [20–23], the others [9,15] concluded that nitrogen is the favourite site. Due to the fact that the calculated energy difference between the two protonated forms is somewhat small and method-dependent, it seems reasonable to admit that both carbon-C_4 and nitrogen protonated isomers are likely to coexist following protonation of aniline.

PAs of the halogeno-anilines have also been investigated in some details. All halogen atoms **X** including F, Cl, Br and I at the *para*-, *meta*- and *ortho*-sites with respect to the amino group have been considered. Results listed in Table 2 were obtained from B3LYP method with 6-31G(d,p) and 6-311++G(d,p) + ZPE. Table 3 records the PAs derived using MP2/6-311++G(d,p) with geometries optimized at the HF/6-31+G(d,p). For the purpose of comparison, the corresponding values from B3LYP method are given in parentheses. It should be stressed that in the present calculations, relativistic effect has not been included in the iodine basis set. Therefore, an additional error of a few kJ/mol on the PAs of iodoanilines could be expected.

As in the case of parent aniline, results derived from molecular orbital MP2 method show again some discrepancies with those given by DFT B3LYP. Thus, in both 3- and 4-halogeno-anilines, protonation takes place at the nitrogen atom according to MP2. In comparison with experimental values of 3-fluoro, 4-fluoro, 3-chloro and 4-chloro given in Table 3, MP2 values have the same trend. The MP2 PAs of 4-halogeno-anilines are larger than those of 3-halogeno-anilines, whereas a reverse conclusion was derived from B3LYP model. Interestingly, the MP2 method also predicts a trend of increasing PAs at the carbon-C_4 of 4-halogeno-anilines when going from F to I, as the B3LYP method does, but these PAs are still smaller than the nitrogen counterparts. Finally, it is remarkable to note that although the two methods show a

Table 3
PAs (kJ/mol, 0 K) of some halogeno-anilines using MP2/6-311++G(d,p)//HF/6-31 + G(d,p) + ZPE

Halogeno-anilines	Proton affinity[a]		
	Nitrogen	Carbon-C_4	Experimental[b]
3-Fluoroaniline	857 (852)	841 (869)	866
4-Fluoroaniline	863 (862)	789 (818)	871
3-Chloroaniline	859 (854)	841 (871)	867
4-Chloroaniline	863 (858)	809 (836)	873
3-Bromoaniline	859 (856)	840 (872)	
4-Bromoaniline	862 (858)	822 (851)	
3-Iodoaniline	860 (859)	840 (875)	
4-Iodoaniline	863 (861)	840 (872)	

[a] Values in parentheses are those obtained from B3LYP/6-311++G(d,p).
[b] Taken from [18].

Table 2
Calculated PAs at 0 K of halogeno(**X**)-anilines (kJ/mol)

Level[a]	Protonation site	Halogeno-anilines											
		X = F			**X** = Cl			**X** = Br			**X** = I		
		C_2	C_3	C_4	C_2	C_3	C_4	C_2	C_3	C_4	C_2	C_3	C_4
I	N	888	880	889	884	876	880	890	879	881	891	881	
	C_4	889	903	843	884	896	859	888	898	877	890	900	
	C_6	870	892	872	867	883	866	871	886	869	874	887	
	C_2	841	883		841	879		854	882		872	884	
II	N	857	852	862	861	854	858	865	856	858	870	859	861
	C_4	857	869	818	858	871	836	861	872	851	866	875	872
	C_6	837	858	840	841	858	840	844	859	842	849	863	847
	C_2	811	849		817	853		814	854		848	858	

[a] Level I = B3LYP/6-31G(d,p) + ZPE. Level II = B3LYP/6-311++G(d,p)//B3LYP/6-31G(d,p) + ZPE. Zero-point energies were obtained from B3LYP/6-31G(d,p).

discrepancy in determining the protonation site of aniline and halogeno-anilines, they agree with each other as far as the values of PAs at nitrogen are concerned. The discrepancy appears mainly on the PA values at the carbon-C_4. In this specific case, the available experimental results appear to support the qualitative predictions made by the molecular orbital methods MP2 and CCSD(T) on the aniline protonation site.

Bearing such differences in mind, it is of interest to make some comments on the results derived from B3LYP computations, in particular on the trends of PAs.

3.2.1.2. 2-Halogeno-anilines. The PAs of 2-halogeno-anilines predicted by B3LYP method have similar values at both nitrogen and carbon-C_4 sites when $\mathbf{X} = \mathrm{F}$ (857 kJ/mol), and are slightly more favoured at nitrogen atom when going from Cl to Br and I by 3–4 kJ/mol. Carbon-C_6 (without halogen substitution) atoms exhibit PAs of about 20 kJ/mol lower with respect to those of carbons-C_4. Protonation at carbon-C_2 (which bears the halogen atom), is less favourable by about 25 kJ/mol relative to the C_6, except when $\mathbf{X} = \mathrm{I}$, where both C_2 and C_6 sites become equivalent. This is in line with the well known fact that the electron-withdrawing effect of iodine is really small. In going from F to I, PAs gradually increase from 857 to 870 kJ/mol for PA(N) and 857 to 866 for PA(C_4) (Table 2, values at B3LYP/6-311++G(d,p) + ZPE).

3.2.1.3. 3-Halogeno-anilines. Experimental observations on the protonation of 3-substituted anilines led to the conclusion that all 3-fluoro and 3-chloroanilines preferably undergo a nitrogen protonation in the gas phase (see [8] for a summary of earlier results). However, the B3LYP PAs reveal rather reverse results. The preferred site of protonation in this case is, according to B3LYP data tabulated in Table 2, the carbon-C_4 associated with PAs of around 16–20 kJ/mol larger than those at nitrogen, irrespective of the nature of the halogen atom. PAs at nitrogen are even smaller than those at the carbon-C_6. As seen in Table 3, the MP2 results indicate a reverse situation in which the nitrogen protonation is clearly favored over carbon-C_4 protonation. As in the case of aniline, the B3LYP model seems to systematically favour the carbon protonation. Thus, a pertinent question is as to whether this case represents a failure of the B3LYP model in predicting PAs.

3.2.1.4. 4-Halogeno-anilines. Results listed in Table 2 show some interesting features for 4-halogeno-anilines. When $\mathbf{X} = \mathrm{F}$, the carbon-C_4 becomes the least favoured site with PAs smaller than those at both *ortho*-carbons (22 kJ/mol) and nitrogen (44 kJ/mol). Nitrogen clearly becomes in this case the most favoured protonation site. However, the gap between both PAs is reduced in going from F to Cl and Br and the situation is reversed following iodine substitution. While PAs at both nitrogen and *ortho*-carbons (C_2 and C_6) remain nearly constant, the PAs of carbon-C_4 increase appreciably from 818 kJ/mol with F, to 836 with Cl, 851 with Br and finally, 872 kJ/mol with I. This shows that halogen atoms at the carbon-C_4 site have strongly reduced, by electron withdrawing effect, their susceptibility to attract a proton. As a result, carbon-C_4 becomes slightly more preferable than nitrogen as a protonation site of 4-iodoaniline whereas nitrogen is the one of 4-fluoro- and 4-chloroanilines. Both sites are more or less competitive in 4-bromoanilines. Again, these results should be regarded with much caution, due to the tendency of B3LYP to overestimate the basicity of carbons-C_4.

3.2.2. Ionization of aniline

In order to determine relative stabilities, a series of isomers of aniline radical cation have theoretically been investigated and the results are summarized in Fig. 4. The distonic isomers **b**, **c**, **d** have been calculated to be 185, 185 and 182 kJ/mol less stable than the conventional aniline radical cation **a**. The energy of transition structure converting the radical cation **d** into **a** by a 1,3-hydrogen shift is relatively high, being 162 kJ/mol above **d**. Interconversions of **b**, **c** and **d** via 1,2-hydrogen shifts within the ring require higher activation energies. Calculated energy barriers for the

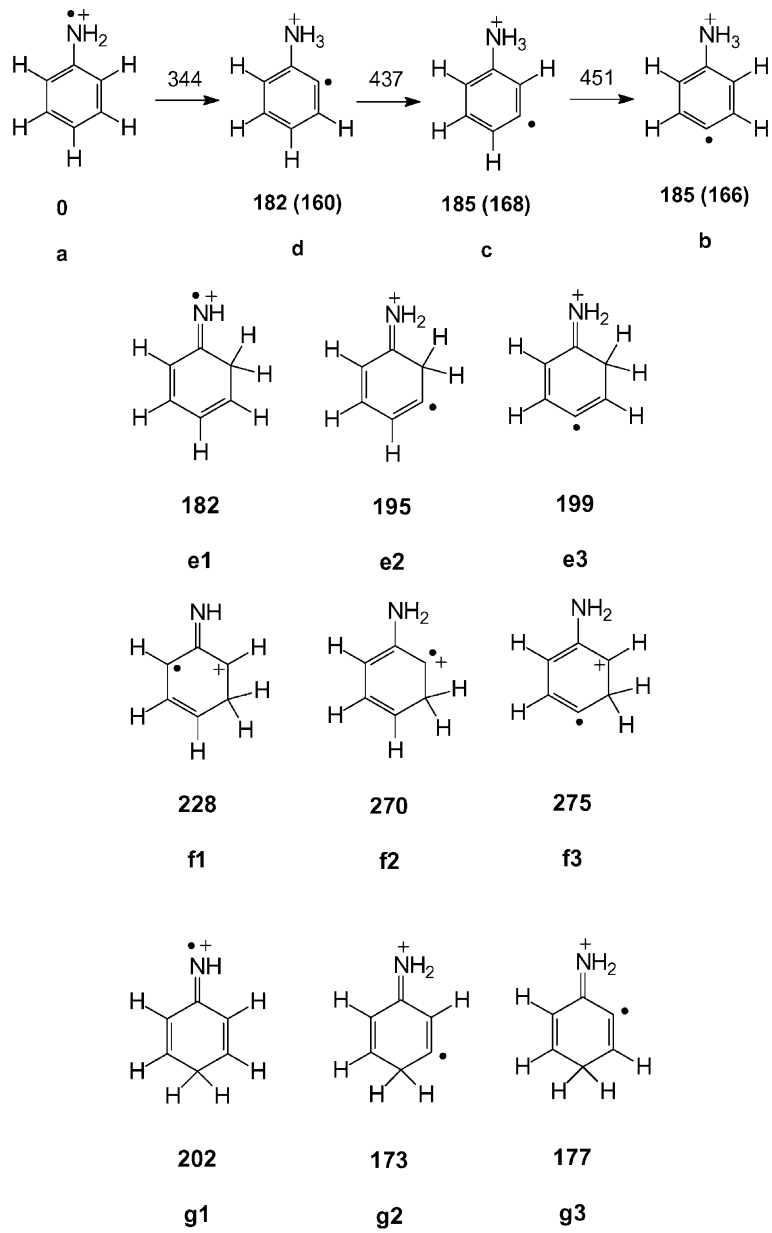

Fig. 4. Relative energies of aniline radical cation isomers (kJ/mol) obtained from B3LYP/6-311++G(d,p) + ZPE. Values given in parentheses were derived from CCSD(T)/6-311++G(d,p) + ZPE. The positions of radical and charge centers are arbitrarily given.

b → **c** and **c** → **d** isomerizations amount to 266 and 252 kJ/mol, respectively. There is no dramatic change in the structure of the distonic isomers **b**, **c** and **d**; the C–N bond length increases from 1.32 Å in the conventional ion **a** to 1.49 Å in the distonic structures. It indicates that a loss of NH_3 should easily be involved in the dissociation of the distonic ions.

For the sake of comparison, other isomeric structures of aniline ion, such as ions **e**(**1**–**3**), **f**(**1**–**3**) and **g**(**1**–**3**) (see Fig. 4), have also been considered. The

Table 4
Dissociation energies (kJ/mol) of the dehalogenation process: *N*-protonated 4-halogeno-anilines → distonic ion **b** + $\mathbf{X}^{\bullet}$

N-protonated, 4-halogeno-anilines	B3LYP/6-31G(d,p) + ZPE	B3LYP/6-311++G(d,p) + ZPE
X = H	473	469
X = F	524	500
X = Cl	370	366
X = Br	342	318
X = I	266	264

relative energies of these ions are likely to be dependent on the position of the sp^3 carbon within the ring. Highest relative energies (228–275 kJ/mol) correspond to the isomers **f1**, **f2** and **f3**, while the lowest involve **g2** and **g3** (173–177 kJ/mol) structures.

For aniline, the adiabatic ionization energy (IE_a) are calculated to be 7.55 and 7.59 eV by the B3LYP and CCSD(T) methods, respectively, using the 6-311++G(d,p) basis set. These values can be compared with the experimental data of 7.72 eV [18].

The C–**X** dissociation energies of *N*-protonated 4-halogeno-anilines are collected in Table 4. The C–**X** bond energies rapidly decrease when going from **X** = F to **X** = I. With a bonding energy of just around 224 kJ/mol, cleavage of a C–I bond in *N*-protonated iodoanilines is apparently readily to take place upon collisional activation giving the distonic isomers **b**, **c** or **d**.

4. Conclusions

In summary, tandem mass spectrometric methodologies have demonstrated that the distonic isomers of ionized aniline are stable species in the gas phase and can be generated by a protonation–deiodination sequence on iodoanilines. Quantum chemical calculations have also indicated that, although the distonic isomers are about 160–180 kJ/mol less stable than ionized aniline, they are protected against hydrogen shifts rearrangements by large energy barriers. This study emphasizes again the remarkable eliminative ability of the iodine atom due to the rather weak C–I bond energies. This could become a quite useful feature in the preparation of less stable isomers of cyclic and/or aromatic derivatives.

Acknowledgements

The Mons laboratory thanks the Fonds National de la Recherche Scientifique (FNRS) for financial support in the acquisition of the large scale tandem mass spectrometer and a postdoctoral fellowship to PG. MTN and HTL are indebted to the KULeuven Research Council (GOA program).

References

[1] L.J. Chyall, H.I. Kenttämaa, J. Am. Chem. Soc. 116 (1994) 3135.
[2] L.J. Chyall, H.I. Kenttämaa, J. Mass Spectrom. 30 (1995) 81.
[3] P. Gerbaux, M. Barbieux-Flammang, Y. Van Haverbeke, R. Flammang, Rapid Commun. Mass Spectrom. 13 (1999) 1707.
[4] R.H. Bateman, J. Brown, M. Lefevere, R. Flammang, Y. Van Haverbeke, Int. J. Mass Spectrom. Ion Proc. 115 (1992) 205.
[5] R. Flammang, Y. Van Haverbeke, C. Braybrook, J. Brown, Rapid Commun. Mass Spectrom. 9 (1995) 975.
[6] (a) M. Polasek, F. Turecek, P. Gerbaux, R. Flammang, J. Phys. Chem. A 105 (2001) 995;
(b) R. Flammang, M. Barbieux-Flammang, E. Gualano, P. Gerbaux, H.T. Le, M.T. Nguyen, F. Turecek, S. Vivekananda, J. Phys. Chem. A 105 (2001) 8579.
[7] N. Russo, M. Toscano, A. Grand, T. Mineva, J. Phys. Chem. A 104 (2000) 4017.
[8] R.K. Roy, F. de Proft, P. Geerlings, J. Phys. Chem. A 102 (1998) 7035.
[9] R.L. Smith, L.J. Chyall, J. Beasley, K.I. Kenttämaa, J. Am. Chem. Soc. 117 (1995) 7971.
[10] S.W. Lee, H. Cox, W.A. Goddard, J.L. Beauchamp, J. Am. Chem. Soc. 122 (2000) 9201.
[11] M.J. Nold, C. Wesdemiotis, J. Mass Spectrom. 31 (1996) 1169.
[12] A.G. Harrison, Y.-P. Tu, Int. J. Mass Spectrom. 195/196 (2000) 33.
[13] Y.K. Lau, P. Kebarle, J. Am. Chem. Soc. 98 (1976) 7452.
[14] C. Fenselau, R.J. Cotter, Chem. Rev. 87 (1987) 501.
[15] Z. Karpas, Z. Berant, R.M. Stimac, Struct. Chem. 1 (1990) 201.
[16] M.J. Frisch, G.W. Trucks, H.B. Schlegel, G.E. Scuseria, M.A. Robb, J.R. Cheeseman, V.G. Zakrzewski, J.A. Montgomery Jr., R.E. Stratmann, J.C. Burant, S. Dapprich, J.M. Millam, A.D. Daniels, K.N. Kudin, M.C. Strain, O. Farkas, J. Tomasi, V. Barone, M. Cossi, R. Cammi, B. Mennucci, C. Pomelli,

C. Adamo, F. Clifford, J. Ochterski, G.A. Petersson, P.Y. Ayala, Q. Cui, K. Morokuma, D.K. Malick, A.D. Rabuck, K. Raghavachari, J.B. Foresman, J. Cioslowski, J.V. Ortiz, A.G. Baboul, B.B. Stefanov, G. Liu, A. Liashenko, P. Piskorz, I. Komaromi, R. Gomperts, R.L. Martin, D.J. Fox, T. Keith, M.A. Al-Laham, C.Y. Peng, A. Nanayakkara, C. Gonzalez, M. Challacombe, P.M. Gill, B. Johnson, W. Chen, M.W. Wong, J.L. Andres, C. Gonzalez, M. Head-Gordon, E.S. Repogle, J.A. Pople, Gaussian 98, Revision A.6, Gaussian Inc., Pittsburgh, PA, 1998.

[17] M.N. Glukhovtsev, A. Pross, M.P. McGrath, L. Random, J. Chem. Phys. 103 (1995) 1878.

[18] S.G. Lias, J.E. Bartmess, J.E.F. Liebman, J.L. Holmes, R.D. Levin, W.G. Mallard, J. Phys. Chem. Ref. Data 17 (Suppl. 1) (1998).

[19] R.W. Taft, Proton Transfer Reaction, E.F. Caldin, V. Gold (Eds.), Wiley, New York, 1975 (Chapter 2).

[20] Y.K. Lau, P. Kebarle, J. Am. Chem. Soc. 98 (1976) 7452.

[21] M.J. Locke, R.L. Hunter, R.T. McIver, J. Am. Chem. Soc. 101 (1979) 272.

[22] K.V. Wood, D.J. Burinsky, D. Cameron, R.G. Cooks, J. Org. Chem. 48 (1983) 5236.

[23] S.J. Pachuta, I. Isern-Flecha, R.G. Cooks, Org. Mass Spectrom. 21 (1986) 1.